Journal of Energetic Materials
Publication details, including instructions for authors and subscription information:
http://www.informaworld.com/smpp/title~content=t713770432

Thermal properties measurements of solid rocket propellant oxidizers and binder materials as a function of temperature

Donna M. Hanson-Parr[a]; Timothy P. Parr[a]
[a] Naval Air Warfare Center Weapons Division, China Lake, CA

To cite this Article Hanson-Parr, Donna M. and Parr, Timothy P.(1999) 'Thermal properties measurements of solid rocket propellant oxidizers and binder materials as a function of temperature', Journal of Energetic Materials, 17: 1, 1 — 48
To link to this Article: DOI: 10.1080/07370659908216094
URL: http://dx.doi.org/10.1080/07370659908216094

THERMAL PROPERTIES MEASUREMENTS OF SOLID ROCKET PROPELLANT OXIDIZERS AND BINDER MATERIALS AS A FUNCTION OF TEMPERATURE

Donna M. Hanson-Parr and Timothy P. Parr
Naval Air Warfare Center Weapons Division
China Lake, CA 93555-6100

ABSTRACT

Using a fairly simple technique and small samples it was possible to obtain thermal diffusivity, specific heat capacity, and thermal conductivity, all as a function of sample temperature, for a variety of ingredients used in solid rocket propellants. The oxidizers AP, ADN, CL20, HMX, RDX, HNF, TNAZ were studied as well as the nonenergetic polymers Teflon™, HTPB, and polyurethane, energetic binders containing GAP and BAMO and/or NMMO, and actual solid propellants XM39, N5, N12, and SB129.

INTRODUCTION

Solid propellant ignition, combustion, and cookoff modeling efforts require thermal properties of materials comprising the propellant as a function of temperature. Measurements have been made for some ingredients in the past. For example, the thermal properties of the oxidizer ammonium perchlorate (AP) are well determined up to 240°C[1-6] Two nitramine oxidizers, RDX[2,3,7-9] and especially HMX[1-4,9-11], have also been studied. These three oxidizers have been used for many years. Some information on binder materials is also available in the literature: for example,

Journal of Energetic Materials Vol. 17, 001-047 (1999)
Published in 1999 by Dowden, Brodman & Devine, Inc.

hydroxy-terminated polybutadiene polymer (HTPB)[3,4] and PEG/BTTN/TMETN[4]. Newer oxidizers have recently been developed, however, for which little thermal properties data are available. It was the goal of this work to obtain thermal properties of these newer materials as a function of temperature.

EXPERIMENTAL

The apparatus used is shown in Fig. 1. The design was based on the "flash heating" concept for measuring thermal diffusivity[1,12(and references therein)-15] wherein a pulse of heat is sent into one face of a thin sample and the temperature rise at the other side is monitored as a function of time.

The sample holder/heater was modular in design. Two Teflon™ rectangular parallelepipeds (boxes) made up the top and bottom pieces of the sample holder, with the sample placed in between the two halves and a type K (chromel-alumel) 5 μm thick foil thermocouple underneath the sample (on top of the bottom piece). On the bottom of the top piece was a 22 μm thick by 620 μm wide chromel foil that was folded back and forth to make a grid that completely covered the sample (about 6mm, see Fig. 1, bottom view). The foil, used for pulse heating the top of the sample, was connected to copper extension wires near the bottom of the top piece. A piece of foil of adequate area to cover the sample was not used because a large enough temperature rise was not achievable due to the too low resistance of the foil (cross

sectional area too large -- see next section). By using the strip of chromel foil, bent back and forth with a tiny space in between folds so that the strips did not touch each other, the resistance was kept high (small cross sectional area) and a large temperature rise was produced. The two sample holder halves slid into a heater block and were tightly clamped together by exerting spring pressure on the top half.

A 80μm layer of Kapton™ was placed between the thermocouple and the bottom Teflon™ block. Between the foil heater and the top Teflon™ block were placed a layer of Kapton™ and a layer of ceramic blanket. These materials were excellent thermal insulators: the thermal conductivity of the ceramic blanket was about 4.2×10^{-4} cal $cm^{-1}s^{-1}°C^{-1}$, compared with about 5×10^{-4} to 10^{-3} cal $cm^{-1}s^{-1}°C^{-1}$ for Teflon™[6], and the thermal diffusivity of the Kapton™ was about 4×10^{-4} cm^2/s, compared with about 10^{-3} cm^2/s for Teflon™[12]. These materials were used to ensure good contact between the foil heater and sample and the sample and thermocouple with minimal heat losses.

The heater block was a chunk of aluminum with a 100W cartridge heater inserted into it, and the heater was plugged into a Variac™ variable transformer. The block was heated to the desired temperature by adjusting the Variac™ and then allowing it to stabilize before doing any measurements. A thermocouple (type J) was inserted into a small hole in the aluminum block to monitor

the block temperature. The other thermocouple (type K foil) was used to measure both the initial sample temperature as well as the temperature rise of the sample after the heating pulse was delivered.

For the thermal diffusivity tests, when a pulse of current was sent through the wire/foil, the foil heated to an estimated Δ T of 72°C during the 1 msec heating pulse (for details see below). Both the temperature rise of the back face of the sample and the current pulse through the foil heater were measured The thermocouple at the bottom of the sample measured the temperature rise as a function of time, and by modeling the system, the thermal diffusivity was obtained. , The signal from this thermocouple was amplified 330 times before sending it through a low-pass filter set at the Nyquist frequency and was amplified an additional 31.6 times (30dB) before going into the A/D digitizer. The sampling rate was usually 2KHz. The current through the foil heater was 8.15 amps for most samples. For samples that had low melting points (like ADN and HNF), a lower heating current was used. A typical temperature rise measured at the back face of the sample was from 0.3°C (low current pulse) to over 2°C (high current pulse). The temperature rise measured depended on several factors as discussed below including thickness of the sample and the amount of heat energy input to the sample. For improved signal to noise at least 5 temperature traces were averaged

together, and for the low temperature rise experiments, up to 10 were averaged.

The samples were either pressed pellets (right circular cylinders) or cured polymeric materials, cut from sheets. The thickness of hard materials was measured directly using a micrometer. Some of the materials resembled gelatin and changed thickness when pressed in the apparatus. For these materials, the thickness was obtained as a difference of the height of the top Teflon™ piece with the sample in place to that with no sample, taking into account the expansion of the Teflon blocks when heated. Sample thickness ranged from about 300μm up to 700μm.

CALCULATIONS

The temperature rise (ΔT_{foil}, °C) obtained during pulse heating depends on the material's resistivity (R_o, Ω-cm), heat capacity ($c_{p,\ foil}$, cal/gm-°C), density (ρ_{foil}, gm/cm^3), and cross sectional area (A, cm^2) and the length of the pulse (Δt, sec) as given by:

$$\Delta T_{foil} = (I^2 R_o \Delta t) / (4.184 \rho_{foil} c_{p,foil} A^2)$$

Therefore, it is important to use something with a high resistivity and small cross sectional area to get a reasonable temperature rise at the other side of the sample and therefore good signal to noise. For chromel, R_o=76.5x10^{-6} Ω-cm, ρ_{foil} = 8.73 g/cm^3, $c_{p,foil}$ = 0.105 cal/gm-°C (actually for nickel). The foil strips had a cross sectional area of 1.36 x 10^{-4} cm^2 (22 μm x

620 μm), the current through the foil was 8.15 amps for 1msec. Therefore, the *expected* temperature rise of the foil heater was 71.6 °C. Temperature rises at the back face of about 1°C were attainable for an 830 μm thick sample of AP.

Since the heating element covered the entire surface of the sample, modeling is essentially one-dimensional. If one calculates the amount of heat going into the sample ($H_0\delta$, H_0, flux in cal/cm^2-s and δ, the pulse duration in sec), measures the maximum temperature rise at the opposite face (ΔT_{max}, °C), and knows the density of the material (ρ, gm/cm^3), and its thickness (L, cm), the specific heat capacity (c_p, cal/gm-°C) can be calculated as follows[14,15]:

$$c_p = (H_0\delta)/(\rho L \Delta T_{max})$$

Since it's difficult to calculate H_0 because the dimensions of the heating foil need to be measured precisely, a sample of known thermal properties can be used as a reference to obtain H_0 experimentally.[15]

Thermal diffusivity (α) can be obtained from the simple relationship[12],

$$\alpha = (1.38\ L^2/\pi^2 t_{1/2}),$$

where $t_{1/2}$ is the time it takes to reach half the maximum temperature rise at the rear face of the sample, if the system is one-dimensional and there are no heat losses with the sample

thermally insulated at the sides and bottom. Here, the sample is not in a vacuum, but instead has air to the sides, Kapton™ at the bottom, and ceramic blanket and Kapton™ above the heating foil, but is one-dimensional.

Another way to obtain α involved fitting the initial temperature rise to a straight line and extrapolating back to a ΔT of 0°C to get t_x. From these results, α was calculated as follows[12]:

$$\alpha = (0.48\ L^2/\pi^2 t_x).$$

Tests were done with thicknesses of AP ranging from 1 mm to 0.6 mm. Using the simple formulae, the derived thermal diffusivities were the same. Therefore, it appears that use of this formula was adequate, i.e. heat losses were not significant. Since the thermal properties of AP[1-6] are well known, it was used as a reference sample to obtain H_0. Any time the foil heater was replaced, a new reference had to be measured, since the foil characteristics would have been different from the previous one.

Calculations were done to verify that use of the simple formula was justified. An example of these results is shown in Fig. 2 for a value of α that was relatively low.

RESULTS AND DISCUSSION

A few simple tests were conducted first to characterize the apparatus. These tests involved putting different materials under the thermocouple to see if the temperature rise of an 830μm thick piece of AP at the back face varied. The materials used in this series of tests were: 1) 80μm thick Kapton™ 2)Kapton™ plus a 375 μm slab of Teflon™, 3) a 375 μm thick piece of Teflon™, 4) AP pellet, and 5) RDX pellet. Within +/- 5%, the temperature rise was the same.

Another series of preliminary tests involved using different thicknesses of AP and obtaining both the temperature rise and thermal diffusivity at room temperature. By using the known value of c_p at room temperature, the heat flux (H_0) was obtained. The value of H_0 obtained for the different tests was essentially the same except for the largest thickness (950μm). This indicates that heat losses were not a factor except for the very thick samples. The density of the thinnest samples (385 and 475 μm) was only 1.72 g/cm^3 (88% TMD), whereas for the others it was 1.88 g/cm^3 (96.4% TMD).

In order to obtain c_p from the temperature rise of the sample, the density of the sample must be known. Table 1 lists all of the materials used and their densities as measured pre-test

or found in the literature. Entries marked "TMD" or "lit" are literature values.

TABLE 1. Materials of This Work

A. Oxidizers	Description	sample density* range (g/cm^3)	TMD*
AP	ammonium perchlorate	1.87-1.89	1.95
HMX	cyclotetramethylene tetranitramine	1.60,1.82	1.90
RDX	cyclotrimethylene trinitramine	1.60-1.64	1.80
ADN	ammonium dinitramide	1.64-1.75	1.8
HNF	hydrazinium nitroformate	1.57,1.81	1.87
CL20	hexanitrohexaazaisowurtzitane	1.84-1.90	1.98
TNAZ	1,3,3-trinitroazetidine	1.65	1.70(est)

B. Polymers		density (g/cm^3)
Teflon™	see text	2.14(meas and lit)
HTPB	hydroxy-terminated polybutadiene	0.88(meas)
poly-BAMO	3,3 bis(azidomethyl)oxetane	1.3(lit)
BAMO/AMMO#		1.26(meas)
NMMO	3-nitratomethyl-3-methyl oxetane	0.84(meas)
BAMO/NMMO/BTTN#		1.35(meas)
GAP gumstock	glycidyl azide polymer	1.22(meas)
GAP/BTTN gumstock		1.43(meas)
GAP azide		1.19(meas)
Polyurethane (PU)		0.95(meas)

C. Propellants		density (g/cm^3)
XM39	see text	1.64(meas)
N5	see text	1.7(meas)
N12	see text	1.6(meas)
SB129	Shuttle Booster Propellant	1.70(meas)*

*:TMD values (g/cm^3) are from the literature, "est" is an estimated value, and "meas" is a measured value of this work. The sample density range is the range of densities of samples of this work.
AMMO is azidomethyl methyl oxetane, BTTN is butanol trinitrate.

An extensive literature search was conducted searching on the key words "thermal properties", "thermal diffusivity", "specific heat capacity", and "thermal conductivity" with the various materials listed in the table above. The DTIC and Chemical Abstracts databases were searched back to around 1960.

Surprisingly little information on thermal diffusivity, thermal conductivity, and specific heat capacity was uncovered.

AP

AP was used as a reference for other materials in order to calculate c_p, as discussed above. The AP powder used to form the pressed cylinders contained crystal sizes on the order of 15-20 μm. Figures 3 and 4 show the results of thermal diffusivity and specific heat capacity measurements, respectively, compared with literature values. Literature values for the specific heat capacity only for room temperature was used to calibrate the instrument in order to obtain $c_p(T)$ for AP as well as other materials. The agreement was excellent when the thermal diffusivity results were corrected for porosity[5] using a β factor of 1.3, such that:

$$(\alpha_{measured}/\alpha_{100\%TMD}) = (1-\beta(1-\rho/\rho_{TMD}))$$

The samples used in the measurements had densities between 96-97% TMD. These samples were obtained from 2mm thick cylinders, pressed neat (no solvent) sanded down to 580 μm. Figure 5 shows the thermal conductivity of AP as a function of temperature, using the measured values of thermal diffusivity (corrected for porosity), specific heat capacity, and density of 1.95 g/cm^3.

Parameters of least squares fits for all of the samples is given in Table 2.

AP has a phase transition temperature of 240°C (orthorhombic to cubic)[5] and starts decomposing if held at this temperature long enough[5]. The densities are 1.957 g/cm^3 and 1.756g/cm^3, respectively for the orthorhombic and cubic phases[3]. Generally, in the current set of tests, the sample was held at a given temperature for about 15 min before proceeding to a higher temperature. For AP above about 225°C, a new, undecomposed piece was used each time. After each test, the apparatus was opened, the thickness of the existing sample was measured, and then the new sample was placed into the apparatus and allowed to warm up to the desired temperature. This warm up process took about 15 min, giving the sample enough time to start decomposing as witnessed by fluctuating temperatures and oxidization of metallic parts of the apparatus. Therefore, measurements above 240°C are suspect and probably not valid due to exotherms (decomposition) and phase changes. The point at very high temperature was from a probably cubic phase piece, but decomposition was probably still progressing. The sample was tightly clamped in place during the temperature increase of the apparatus, causing further constriction as the Teflon™ pieces expanded with temperature. Near the phase change temperature, the sample was first observed to be substantially thicker and then thinner again at higher

temperatures. For example, an initially 580 μm thick sample swelled to 630 μm at 240°C and remained that thickness when cooled to room temperature. A sample initially at 585 μm was only 440 μm post-test after having been heated to 264°C.

The agreement with various literature results is good. The thermal diffusivity (and conductivities) of Shoemaker, et.al.[3] are somewhat lower than the current results. The authors remarked in their paper that these values (for single crystals) are too low, however.

HMX

Samples of densities 96%TMD and 84% TMD were used to obtain thermal diffusivity and specific heat capacity from room temperature up to 240°C for HMX. The powder used to press the cylinders was military grade HMX (containing 0.21% RDX) of about 75 μm particle size. One drop of acetone was using during the pressing process, and the samples were vacuum dried at about 80°C prior to use. The higher density samples were obtained from 2mm thick cylinders, sanded down to 580 μm. The lower density samples were used as pressed (about 500μm thick). Thermal conductivity as a function of temperature was subsequently calculated from the diffusivity, heat capacity and density. For samples above about 170°C, the thickness had to be measured after each test. Due to the phase change from the β to the δ polymorph above this

temperature, the sample thickness was seen to significantly increase, similar to what was seen for AP above. The sample density was also remeasured for each of these tests. TMD for the δ-polymorph is only 1.8 g/cm^3, compared with 1.9 g/cm^3 for the β-polymorph.[2] Notable decomposition was observed above about 220°C as evidenced by measurable mass loss, a change in color from white to brownish, and a decrease in the sample thickness.

To correct the thermal diffusivity for porosity, the simple method of just dividing by (1-porosity) was used in lieu of something similar to the treatment for AP. With this simple correction, thermal diffusivities from the 96% vs. 84% TMD samples agreed well within experimental reproducibility. Therefore, a more elaborate treatment didn't appear to be warranted. As seen in Fig. 6, current thermal diffusivity results compared well with those measured in 1983 in this laboratory[1], and the value at room temperature agrees with the results from the Lawrence Livermore National Laboratory (LLNL) handbook[2]. The values of Stokes, et.al.[4] and Shoemaker, et.al.[3] are substantially lower than the current results. The LLNL values as well as those shown for Stokes, et al and Shoemaker, et al were derived from given values of c_p and k. Shoemaker, et.al measured thermal conductivity of HMX powder and then corrected for porosity. The authors did not state what the density of the powder was nor how the correction for porosity was handled.

Fig. 7 shows the specific heat capacity obtained for HMX. Here, the actual sample density was used in the calculations, not the TMD. There is excellent agreement with various literature results up to about the temperature at which the phase change occurs. At this point, the current results increase very rapidly with increasing temperature while those of Shoemaker, et.al.[3] and Rogers (referenced in the LLNL handbook, ref. 2) do not. The two points above 170°C were measured very carefully as discussed above: however, if any endo- or exotherms are present, the results would become invalid since the determination of c_p depends on the temperature rise measured. As seen in the LLNL handbook HMX exhibits an endotherm associated with the β-δ phase change. With such an endotherm, the measured temperature would be lowered and the subsequent c_p calculated from the temperature rise would therefore appear too large. The points shown for temperatures above 175°C were for tests in which the sample was held at that temperature for about an hour prior to pulsing the foil heater. For earlier tests in which the samples were held at temperature for about 15 min the c_p obtained was even higher and the sample thickness also larger, indicating that the phase transformation was in progress. It was hoped that by holding the sample for an hour above the phase transformation temperature that the sample would have totally converted to the delta phase before the test. Apparently that was not the case. Some deviation is seen in two

points below 175 °C. This may be due to endotherms at the sample surface during the foil heater pulse.

The thermal conductivity, k, for HMX is shown in Fig. 8, obtained by multiplying the thermal diffusivity (corrected for porosity) times the TMD times the specific heat capacity. There is a lot of scatter among literature values at ambient temperature and the current data is well within that range. It is seen that k decreases with temperature, in agreement with the results of Shoemaker, et.al.[3] Since the c_p values obtained above (current work) were too high above 175°C, the k values in Fig. 8 are also too large above 175°C.

RDX

The samples of RDX were made using powder of approximately 15 μm average particle size pressed to 89 - 91% TMD using 1 drop of acetone to form 500 μm thick cylinders. The samples were dried prior to use. Attempts to make higher density samples of 580 μm thickness from originally 2mm thick samples failed. The material crushed into powder too easily. Figures 9-11 show the thermal diffusivity, specific heat capacity and thermal conductivity for RDX as a function of temperature. The values were corrected for porosity using the simple methods as done for HMX.

The specific heat data are in excellent agreement with the literature. The thermal diffusivity (and, therefore, thermal conductivity) values are somewhat higher than those of Miller[8] and especially higher than those of Shoemaker, et al[3]. As seen above for AP and HMX, the thermal conductivities given in the paper by Shoemaker, et al were also lower than the results presented here. Shoemaker, et al[3] state in their paper that the values shown for the *pressed* AP powder was much too low, compared with their *single crystal* results. Perhaps the same problem existed for the pressed HMX and RDX powders. The RDX used here was military grade, used as received, which contained about 5.5% HMX. Since HMX has a much higher thermal diffusivity than RDX, the higher diffusivities of the RDX over literature could in part be due to the HMX. The RDX used by Miller[8] contained only 1% HMX. The correction for porosity used here was the same as for HMX (dividing by the fraction TMD of the density). Since HMX and RDX have essentially identical specific heat capacities, the fact that the RDX contained some HMX did not affect those results.

Oxidizers ADN, CL20, HNF, and TNAZ

Oxidizers that have been developed more recently than AP, HMX, and RDX have very little or no thermal properties data available in the literature.

The ADN was from SRI-12 lot PRD50-24. The pressed pellets were at least a year old and had been kept in a desiccator in the dark.

The TNAZ was obtained from NAWCWPNS. It looked brownish on top after being heated to 81°C. TNAZ melts at 100°C, so the browning at the surface of the sample was probably due to the foil heater pulse.

The CL20 was from SRI, lot# unknown, but one in which the CL20 looked white, not yellowish. The CL20 looked intact post-test after being heated to 192°C, but turned tannish-yellow, and turned very brown if left for a long time at 220°C. CL20 exothermically decomposes starting at 165°C, peaking at 239°C.[16]

The HNF was obtained from Edwards Air Force Base, but was originally synthesized by Rocketdyne about 20 years ago and stored in CCl_4. Recent tests in this laboratory were conducted to measure the melting point of this HNF because impurities would decrease it. The melting point obtained was 117°C - 118°C, close to the temperature at which the pure material melts. The sample was seen to be discolored after removing it from the apparatus after having been heated to 108°C.

The samples used here were pressed cylinders, all of which were pressed without the use of a solvent. The denser samples

were from originally 2mm thick cylinders sanded down to 580 μm. About half of the HNF points are from 84% TMD dense samples, but the rest are from 97% TMD ones. The ADN samples were from 91 - 97% TMD. The CL20 were in the 93-96% TMD range, and the TNAZ was 97% TMD. For the low melting materials, the foil heater current was reduced so that the sample would not melt prematurely. Figs. 12 - 14 show the results obtained. Included in the figures are least-squares linear fits for AP, HMX, and RDX, shown for comparison.

The thermal conductivities of HNF, RDX, CL20, and TNAZ all appear to be about the same. Those for AP, ADN, and HMX are considerably higher. There's a fair amount of scatter associated with the measurements of HNF and ADN. To correct the results for porosity, the thermal diffusivity (and, therefore conductivity) was simply divided by the fraction TMD of the sample density. It was seen for AP[5] that this simple correction was not adequate. The thermal diffusivity of HNF obtained using the present techniques is somewhat lower than what was obtained by fitting thermocouple measurements of a sample burning at atmospheric pressure.[17] Those fits yielded an average α of from 2.1×10^{-3} to 2.2×10^{-3} cm^2/s.

Teflon™, HTPB, and Polyurethane

Teflon™ was used as a kind of standard. There is quite a bit of information on the thermal diffusivity in the literature[12], and it has low values of thermal diffusivity and conductivity. The sample used here was cut from a 375μm thick smooth sheet. Figs. 15 through 20 show the results for Teflon™ as well as for HTPB and polyurethane.

Teflon™ undergoes a crystal-crystal transition near 25°C, so the values of this work near that temperature may be suspect. Therefore, the linear fits shown (this work) do not include the value at room temperature. As can be seen in the figures, there is good agreement with literature values of thermal diffusivity, considering the amount of scatter in the literature curves. There is excellent agreement with the one specific heat capacity literature point[18] at 60°C, and excellent agreement with the thermal conductivity literature numbers. Teflon™ is also known as: tetrafluoroethylene (TFE), polytetrafluoroethylene (PTFE), and fluorinated ethylene-propylene (FEP) resin.

The HTPB used in the current work was R45M with N100 curative. The resulting material was translucent with essentially no color, pliable, and didn't crumble when pressure was exerted on it. A piece that looked bubble-free was used. Figs. 16, 17, and 19 show the results compared with literature values. The

agreement with Shoemaker, who did thermal diffusivity and conductivity as a function of temperature, was excellent. Agreement with literature values of c_p are also excellent[4,19]. After being heated to 178°C, the HTPB sample turned very dark orange and became very crumbly.

The polyurethane used was mixed from a commercial package (urethane polymer + polymeric isocyanate) and then allowed to cure at room temperature for at least a day, so that it was no longer sticky. Samples which looked bubble-free were used. The material was very pliable yet stiff enough so that the sample thickness did not diminish when clamped into place in the apparatus. The melting point of this material was somewhere between 198°C and 235 °C.

Literature data of thermal properties of polyurethane are often for very low density foam material. The thermal conductivity for *solid* polyurethane is cited in ref. 20. Figs. 16, 17, and 20 show the current results. The agreement with the one literature point for thermal conductivity is good, considering there is a lot of scatter associated with this number[20].

Energetic binders: GAP-containing.

Figs. 21 through 23 show the results for a set of three polymers all containing GAP. The sample called GAP gumstock is 100% GAP triol polymer, GAP/BTTN gumstock is 46% GAP and 50% BTTN

with about 4% HMDI and an NCO-OH of 1.2, and GAP azide was about 11% GAP triol, 80% GAP azide, 3% N-100, and 6.5% of PCP. These samples were made by NAWCWPNS/China Lake personnel specializing in propellant manufacture.

The GAP azide material apparently has the highest thermal diffusivity, specific heat capacity, and thermal conductivity of all three, but appears to start decomposing at a somewhat lower temperature. GAP starts to decompose around 150°C, according to one report[21], while another[22] reports primary decomposition at 120 °C, and most others[22] report decomposition above 200°C. Oyumi[23] reports a 9.1% weight loss of GAP-azide at 160°C (after more than 2 hours).

It was observed that the thickness of the GAP gumstock remained the same with temperature up until about 187°C. At this temperature only a charred piece remained. The GAP azide sample held it's shape well until it was definitely melted (or, the viscosity was such that the material flowed away from the sample holder) from 159°C to 173°C, and had completely disappeared by 186° C. The GAP/BTTN gumstock appeared to soften considerably between 120°C and 154°C, as seen by a substantial reduction in the sample thickness.

Energetic Binders: BAMO and/or NMMO-containing.

Results of poly-BAMO and poly-NMMO as well as two combinations (BAMO/AMMO and BAMO/NMMO/BTTN) are presented in Figs. 24-26. The BAMO/AMMO from Thiokol was 35% BAMO. The BAMO/NMMO/BTTN gumstock was about 18% BAMO/NMMO, 61.5% BTTN, 18.5% TMETN, and 2% N-100. Samples of BAMO/AMMO, which started to melt somewhere between 71°C and 78.5°C, were made by heating some to 100°C and then flattening it out to the desired thickness while keeping it flat, and then cooling. The poly-BAMO samples, which started to melt around 74°C, were also formed in this way. The NMMO, cured at least a year ago, was clear and soft like gelatin, and was very sticky. The NMMO melted somewhere between 90 and 100 °C.

A 5μm-thick sheet of Mylar™ was used to wrap around these materials to keep them from sticking to parts of the apparatus. Separate tests using AP and Teflon™ showed that using Mylar™ did not affect the results within experimental error. The sample thickness was very dependent on how tightly clamped the apparatus was, and, since the tightly clamped Teflon™ blocks expanded when heated, the sample thicknesses decreased with increasing temperature. The curves labeled "new" and "old" poly-BAMO were from two different samples: the "old" was poly-BAMO that was in our possession for about a year, and the "new" BAMO was just acquired poly-BAMO. Within the limits of the data scatter, the

results appear to be the same. The BAMO/NMMO/BTTN sample crumbled when compressed, so only points at 21°C and 25°C were obtained. For the other materials, over the small temperature range sampled, the results looked relatively flat.

Based on the results of the pure materials in conjunction with the mixtures, using an additive law, it can be seen that AMMO has about the same c_p as NMMO, and BTTN has a very low c_p value. AMMO appears to have a *very* low thermal diffusivity, much lower than that for NMMO, while that for BTTN appears very high.

Generally thermal diffusivity decreases with increasing temperature, but for NMMO it appeared to increase. The specific heat capacities of all the BAMO- and/or NMMO-based polymers appeared to decrease with temperature instead of increase. Because of the way the sample thickness had to be measured, an error of only 50μm too large (about the accuracy of the technique to measure thickness while the sample was inside the apparatus) could account for these results, especially since the samples were on the order of only 250 μm at the higher temperatures.

Propellants: XM39, N5, N12, SB129

Several propellants were included in this study for comparison purposes. The percentages to follow are weight%. XM39 is a nitramine-based gun propellant containing 76% RDX, 12%

cellulose acetate butyrate, 4% nitrocellulose, 7.6% acetyl triethyl citrate, and 0.4% ethyl centralite[24]. N5 and N12 are double-base propellants. SB129 (shuttle booster) contained about 70% AP, 16% Al, and 14% PBAN binder. Samples of these materials were obtained by microtoming approximately 500 μm thick slices off thicker samples.

The N5 and N12 samples were quite stiff and unyielding to the apparatus clamp-down pressure, so the sample thickness was measured with a micrometer prior to placing into the apparatus. When the temperature of the N5 reached about 92°C a glitch in the thermocouple trace at time zero appeared. Upon opening the apparatus, the sample looked shiny as though some liquid material had come out of the matrix. N12 is N5 without the lead additive, but because it was black instead of red like N5, it may have contained some carbon black. Measurements only at room temperature were made for N12.

XM39 softened considerably with increasing temperature and the sample thickness grew thinner as the Teflon™ blocks expanded. Therefore, when the sample thickness grew too thin, a fresh piece was used. The sample thickness had to be measured post-test with a micrometer at each temperature in order to get meaningful results. The sample turned a tannish-yellow color around 147°C.

SB129 also softened with temperature and examination of the sample post-test at 192°C showed that the sample had turned very dark and was difficult to remove from the foil. A large glitch at time zero was also present, possibly indicating that some part of the propellant was degrading.

Figures 27 through 29 show the results for these four propellants. The data scatter for the aluminized propellant can be seen in the figures, and amounted to about +/- 15%. The only literature values with which to compare were those of Miller[24], who did measurements on XM39. The comparison is good within the mutual temperature range. N12 did not appear to have the same thermal diffusivity or specific heat capacity as N5, but did have the same thermal conductivity. N12 had a higher thermal diffusivity but a lower specific heat capacity than N5. Their densities were close in value to each other (Table 1).

As a check of the technique's accuracy, values for α, c_p, and k for SB129 can be estimated by summing relative contributions of each material.

For the specific heat capacity, molar contributions are summed to get the mixture specific heat capacity: $c_p = \Sigma(c_p * X)_i$.

For thermal conductivity (and, diffusivity) obtaining an estimate is not straight-forward[18], but a simple formula (molar rule of mixtures) can be tried[18]:

$k(or, \alpha) \approx (\Sigma(X_i/k_i))^{-1}$ for i components, where X_i is the *mole* fraction of component i, or

$$X_i = ((\text{weight\%})_i/MW_i)/\Sigma((\text{weight\%})_i/MW_i).$$

At 21°C, from the results presented above (using results of HTPB instead of PBAN, which was not measured):

AP: α = 0.0025 cm^2/s, c_p (literature)=0.265 cal g^{-1} $°C^{-1}$, and k = 0.00127 cal cm^{-1} s^{-1} $°C^{-1}$

HTPB: α = 0.00108 cm^2/s, c_p =0.51 cal g^{-1} $°C^{-1}$, and k = 0.00048 cal cm^{-1} s^{-1} $°C^{-1}$

Al (ref. 4): α = 0.496 cm^2/s, c_p = 0.215 cal g^{-1} $°C^{-1}$, and k = 0.289 cal cm^{-1} s^{-1} $°C^{-1}$

Densities used for AP and HTPB were listed in Table 1, and ρ_{Al} = 2.7g/cm^3. Molecular weights are: 27g/mole for Al, 117.5 g/mole for AP, and about 52 g/mole for HTPB (monomer unit, or EW=1250g/mole).

	α^* (cm^2/s)	c_p^* (cal g^{-1} $°C^{-1}$)	k^* (calcm$^{-1}s^{-1}°C^{-1}$)
Calculated:	0.0048-0.0030	0.242-0.290	0.00243-0.00141
Measured:	0.00274	0.254	0.00129

* For the calculations, the first number is using 1250g/mole for HTPB and the second is using 52g/mole.

The c_p values measured match the predicted ones very well. The α and k values are also very close, using the HTPB monomer unit molecular weight, considering the crude method of calculating them, and using the values of HTPB for the PBAN binder.

CONCLUSIONS

Temperature-dependent thermal diffusivity, specific heat capacity, and thermal conductivity were obtained for the oxidizers AP, ADN, CL20, HMX, RDX, HNF, and TNAZ, the nonenergetic polymers Teflon™, HTPB, and polyurethane, energetic binders containing GAP and BAMO

and/or NMMO, and actual solid propellants XM39, N5, N12, and SB129. Where literature values existed, agreement with current results was good to excellent in most cases.

Using a one-dimensional apparatus greatly simplified the analysis, especially since the heat losses were found to be negligible in the time frame of the experiment.

All DATA SUMMARY

A summary of results is given in Table 2 in the form of straight-line fits to the data (in all but one case). Note the temperature range of validity of these fits.

TABLE 2. Fits to This Work ($x = a_0 + a_1 * T(°C)$, $x = \alpha$, c_p, or k)

2A. Thermal Diffusivity, α (cm^2/s).

	a_0	a_1	T(°C) range
A. Oxidizers			
AP	2.58E-3	-4.54E-6	20-214
HMX	2.62E-3	-6.74E-6	20-170
RDX	1.52E-3	-3.70E-6	20-150
ADN	1.89E-3	-1.74E-6	20-65
HNF	1.88E-3	0	20-110
CL20	1.43E-3	-3.92E-6	20-190
TNAZ	1.51E-3	-3.36E-6	20-88
B. Polymers			
Teflon™	1.31E-3	-1.56E-6	60-162
HTPB	1.08E-3	-1.15E-6	20-180
poly-BAMO	1.62E-3	-4.27E-6	20-74
BAMO/AMMO	0.85E-3	-0.386E-6	20-70
NMMO	0.98E-3	4.54E-6	20-90
BAMO/NMMO/BTTN	1.90E3	0	20-25
GAP gumstock	1.20E-3	-3.93E-6	20-190
GAP/BTTN	1.00E-3	-2.01E-6	20-155
GAP azide	1.43E-3	-2.81E-6	20-105
Polyurethane	1.33E-3	-0.607E-6	20-200
C. Propellants			
XM39	1.38E-3	-2.47E-6	20-145
N5	0.955E-3	-0.914E-6	20-92
N12	1.25E-3		20
SB129	2.91E-3	-4.41E-6	20-192

2B. Specific Heat Capacity (cal $g^{-1}°C^{-1}$)

	a_0	a_1	T(°C) range
A. Oxidizers			
AP	0.251	4.076E-4	20-214
HMX	0.230	6.60 E-4	20-170
RDX	0.235	8.43E-4	20-150
ADN	0.308	3.61E-4	20-65
HNF	0.198	3.41E-4	20-110
CL20	0.238	7.52E-4	20-190
TNAZ	0.328	0E-4	20-88
B. Polymers			
Teflon™	0.208	5.80E-4	60-162
HTPB	0.486	8.49E-4	20-180
poly-BAMO	0.368	-3.04E-4	20-74
BAMO/AMMO	0.594	-15.0E-4	20-70
NMMO	0.684	-11.8E-4	20-90
BAMO/NMMO/BTTN	0.228	0	20-25
GAP gumstock	0.414	9.66E-4	20-190
GAP/BTTN	0.328	5.10E-4	20-155
GAP azide	0.519	2.15E-4	20-10

2B. (continued) Specific Heat Capacity (cal $g^{-1}°C^{-1}$)

	a_0	a_1	T(°C) range
Polyurethane	0.270	21.3E-4	20-200
C. Propellants			
XM39	0.296	0.805E-4	20-145
N5	0.299	2.38E-4	20-92
N12	0.258	----------	20
SB129	0.254	9.86E-4	20-192

2C. Thermal Conductivity, k (cal cm^{-1} s^{-1} $°C^{-1}$).

	a_0	a_1	T(°C) range
A. Oxidizers			
AP	1.285E-3	-9.2E-7	20-214
HMX	1.19E-3	-11.5E-7	20-170
RDX	0.665E-3	0	20-150
ADN	1.08E-3	-5.78E-7	20-65
HNF	0.686E-3	0	20-110
CL20	0.744E-3	-9.33E-7	20-190
TNAZ	0.841E-3	-25.7E-7	20-88
B. Polymers			
Teflon™	0.59E-3	4.8E-7	60-162
HTPB	0.472E-3	1.33E-7	20-180
poly-BAMO	0.739E-3	-14.1E-7	20-74
BAMO/AMMO	0.63E-3	-18.2E-7	20-70
NMMO	0.57E-3	12.3E-7	20-90
BAMO/NMMO/BTTN	0.87E3	0	20-25
GAP gumstock	0.65E-3	-14.6E-7	20-190
GAP/BTTN	0.44E-3	-1.67E-7	20-155
GAP azide	0.89E-3	-14.4E-7	20-105
Polyurethane	0.51E-3	12.8E-7	20-200
C. Propellants			
XM39	0.636E-3	-1.157E-7	20-145
N5	0.487E-3	1.23E-7	20-92
N12	0.521E-3	----------	20
SB129	1.300E-3	1.57E-6	20-192

ACKNOWLEDGMENTS

We wish to thank Dr. Jay Levine of Phillips Laboratory for the HNF, Vicki Brady, Dr. May Chan, and Dr. Russ Reed of NAWCWPNS/China Lake for the GAP-containing materials and pure poly-BAMO, Dr. Fred Blomshield and Jerry Finlinson of

NAWCWPNS/China Lake for the SB129 and GAP gumstocks, Dr. Martin Miller of ARL for the XM39, Dr. Gerry Manser of Aerojet for pure poly-BAMO and CL20, Dr. Richard Hollins of NAWCWPNS/China Lake for the TNAZ, SRI for the ADN, Thiokol for the BAMO/AMMO, and especially Dr. Richard Miller of ONR for funding this work.

REFERENCES

1. D.M. Parr and T.P. Parr, "Condensed Phase Temperature Profiles in Deflagrating HMX", in Proceedings of the 20th JANNAF Combustion Subcommittee Meeting, Vol. I., pp. 281-291 (1983). CPIA pub. 383.

2. Brigitta M. Dobratz, ed. "Properties of Chemical Explosives and Explosive Simulants", Lawrence Livermore Laboratory report number UCRL-51319 Rev.1., July 31, 1974, also, same title, Brigitta M. Dobratz and P.C. Crawford, eds., UCRL-52997, Change 2., 1985.

3. Robert L. Shoemaker, John A. Stark, Raymond E. Taylor, "Thermophysical properties of propellants", in High Temperatures-High Pressures, vol. 17, pp. 429-435, 1985, . 9 ETPC Proceedings page 423.

4. B.B. Stokes, D.W. Booth, and R.E. Askins, "Influence of Physicochemical Properties of Ingredients on Burning Rate Temperature Sensitivity of Solid Propellants", in Proceedings of the 22nd JANNAF Combustion Subcommittee Meeting, Vol. II., p. 97 (1985). CPIA pub. 432.

5. W.A. Rosser, S.H. Inami, and H. Wise, "Thermal Diffusivity of Ammonium Perchlorate", AIAA J 4, 663 (1966).

6. Y.S. Touloukian, R.W. Powell, C.Y. Ho, and P.G. Klemens, "Thermal Physical Properties of Matter, Volume 2. Thermal Conductivity, Nonmetallic Solids" (IFI/Plenum, New York, 1970).

7. J.T. Rogers (compiler), "Physical and Chemical Properties of RDX and HMX", Holston Defense Corporation, August 1962. Control No. 20-P-26 Series B.

8. Martin S. Miller, "Thermophysical Properties of RDX", Army Research Laboratory report, ARL-TR-1319, March 1997.

9. B.D. Smith, M.S. Ramsburg, and J. M. Harrison, "Specific Heats of HMX and RDX by the Differential Scanning Calorimetric Technique", U.S. Naval Weapons Laboratory report, TR-2475, September 1970.

10. L.G. Koshigoe, R.L. Shoemaker, and R.E. Taylor, Specific Heat of Octahydro-1,3,5,7-Tetranitro-1,3,5,7-Tetrazocine (HMX)", A special report to AFOSR, TPRL 314. Jan. 1983.

11. L.G. Koshigoe, R.L. Shoemaker, and R.E. Taylor, Specific Heat of HMX", AIAA J. 22, 1600 (1984).

12. Y.S. Touloukian, R.W. Powell, C.Y. Ho, and M.C. Nicolaou, "Thermal Physical Properties of Matter, Volume 10. Thermal Diffusivity" (IFI/Plenum, New York, 1973).

13. H.S. Carslaw and J.C. Jaeger, "Conduction of Heat in Solids" (Oxford University Press, New York, 1959), 2nd ed., p. 101.

14. W.J. Parker, R.J. Jenkins, C.P. Butler, and G.L Abbott, "Flash Method of Determining Thermal Diffusivity, Heat Capacity, and Thermal Conductivity", J. Appl. Phys. 32(9), 1679 (1961).

15. K. Kobayasi, "Simultaneous Measurement of Thermal Diffusivity and Specific Heat at High Temperatures by a Single Rectangular Pulse Heating Method", Int. J. Thermophys., 7(1), 181 (1986).

16. A.I. Atwood, M.L. Chan, R.A. Hollins, K.J. Kraeutle, T.P. Parr, R. Reed, Jr,, "Synthesis and Characterization of New Energetic Materials: Key to Future Propellants and Explosives", in IR&IED Annual Report 1993, Naval Air Warfare Center Weapons Division, China Lake Report NCWPNS TP 8 182.

17. J. Louwers, "HNF Combustion and Decomposition Experiments: UV-Absorption, Thermal Profile, PLIF", TNO Report PML 1997-C41.

18. J.F. Drolet, "Castable Composite Explosives: Specific Heat at Constant Pressure", Defense Research Establishment Valcartier (DREV) report, DREV TN-2023/73, Feb. 1973.

19. F.A. Christie and J.F. Drolet, "Castable Composite Explosives: Evaluation of Thermophysical Properties", Defense Research Establishment Valcartier (DREV) report, DREV TN-2057/73, April 1973.

20. P.G. Collishaw and J.R.G. Evans, "An Assessment of Expressions for the Apparent Thermal Conductivity of Cellular Materials", J. Materials Sci. 29, 486-498 (1994).

21. Berge B. Goshgarian, "The Mechanism of Nitramine and Advanced Propellant Ingredient Initial Thermochemical Decomposition", Air Force Rocket Propulsion Report, AFRPL-TR-82-040, June 1982.

22. A.N. Nazare, S.N. Asthana, and Haridwar Singh, "Glycidyl Azide Polymer (GAP) -- An Energetic Component of Advanced Solid Rocket Propellants -- A Review", J. Energetic Materials 10, 43-63 (1992).

23. Yoshio Oyumi, "Thermal Decomposition of Azide Polymers", Propellants, Explosives, Pyrotechnics, 17, 226-231 (1992).

24. Martin S. Miller, "Thermophysical Properties of Six Solid Gun Propellants", Army Research Laboratory report, ARL-TR-1322, March 1997. (XM39)

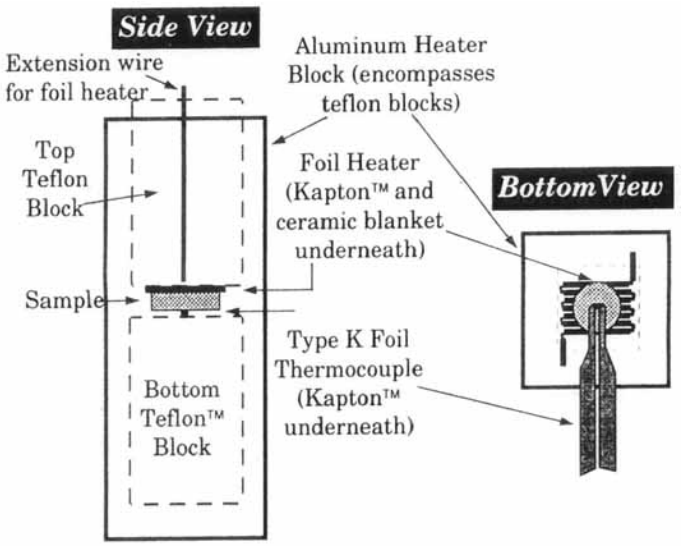

FIGURE 1.

Apparatus used to measure thermal diffusivity. The widths of the foil heater and thermocouple (side view) and the spaces between foil segments (bottom view) are exaggerated for clarity. The butt-welded junction of the foil thermocouple was 5 μm thick and was positioned at the center of the sample.

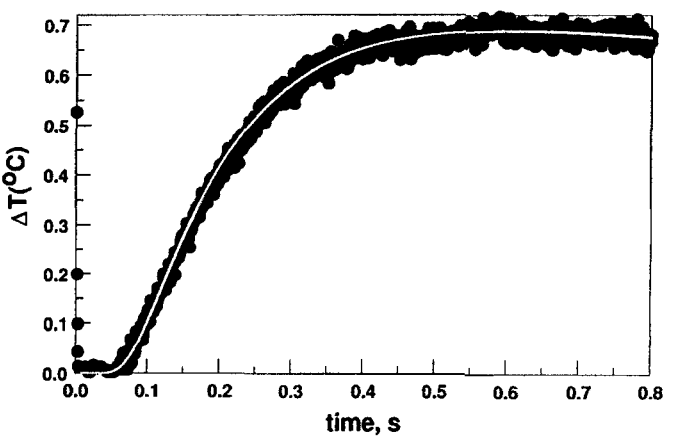

FIGURE 2.

Example fit to time vs. temperature rise plot used to determine the thermal diffusivity, α. For this curve, α was 1.12 x 10^{-3} cm^2/s, with a $t_{1/2}$ = 175 ms, and sample thickness of 375 μm. Circle = data, line = fit.

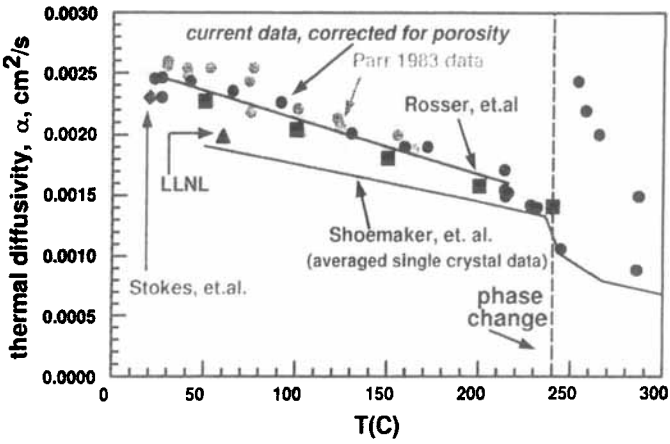

FIGURE 3.
Thermal diffusivity of AP as a function of temperature.

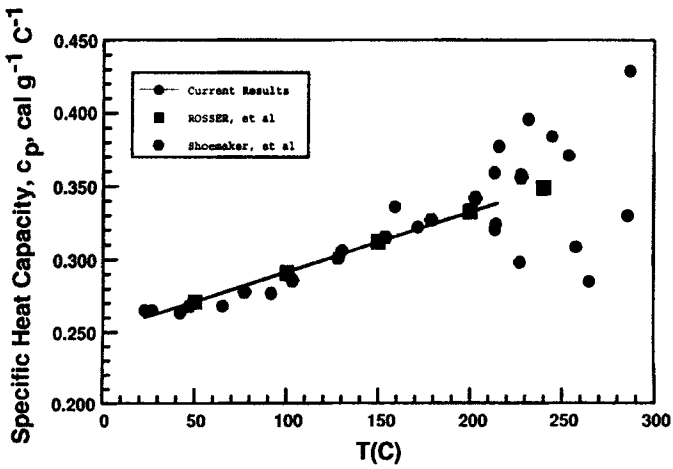

FIGURE 4.
Specific heat capacity of AP as a function of temperature.

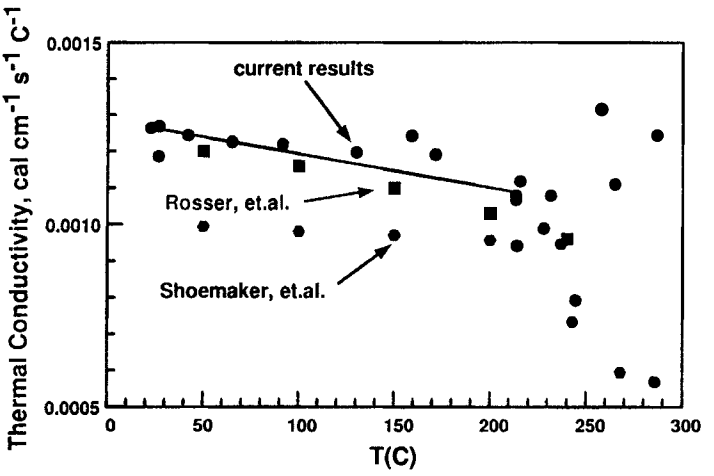

FIGURE 5.
Thermal conductivity of AP as a function of temperature.

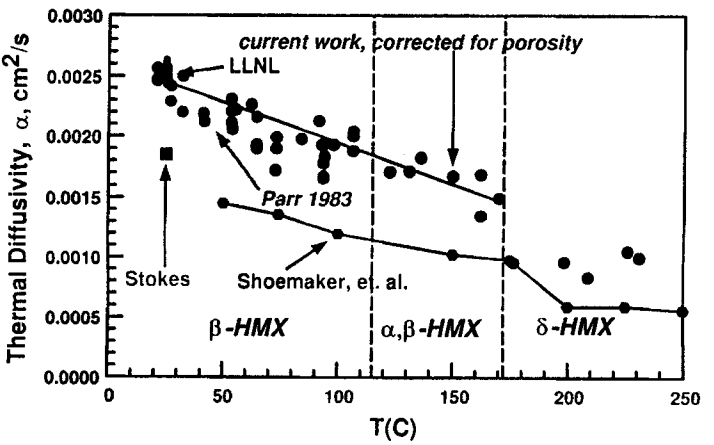

FIGURE 6.
Thermal diffusivity of HMX

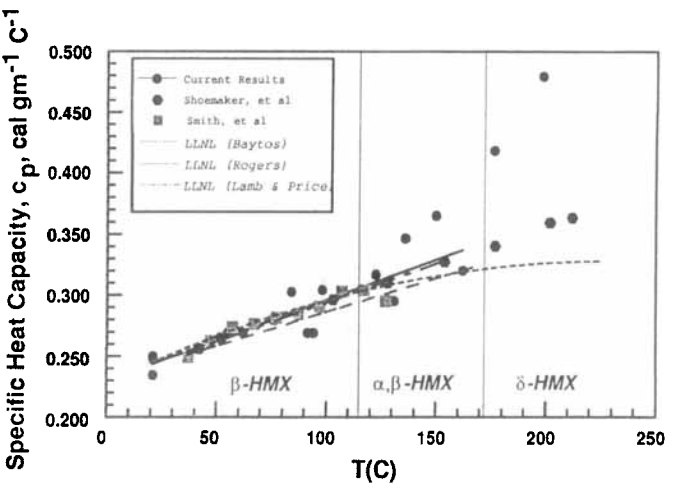

FIGURE 7.
Specific heat capacity results for HMX.

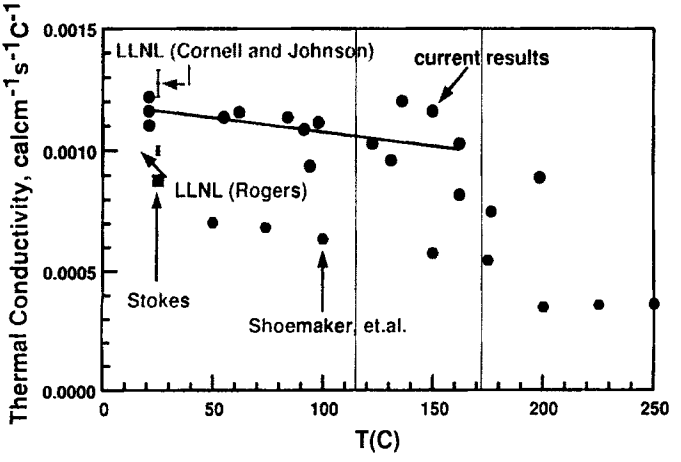

FIGURE 8.
Thermal conductivity for HMX.

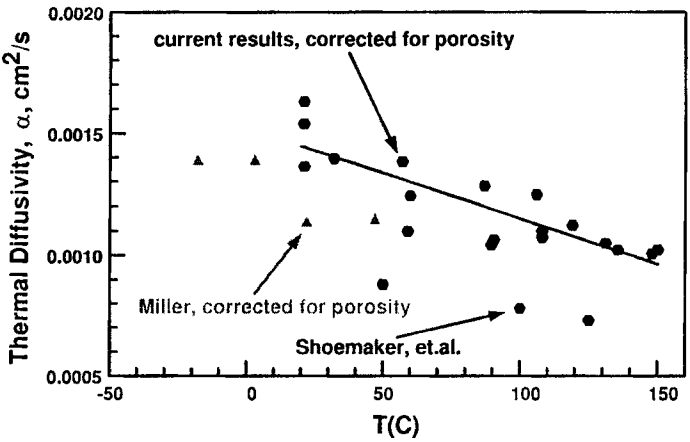

FIGURE 9.

Thermal Diffusivity of RDX.

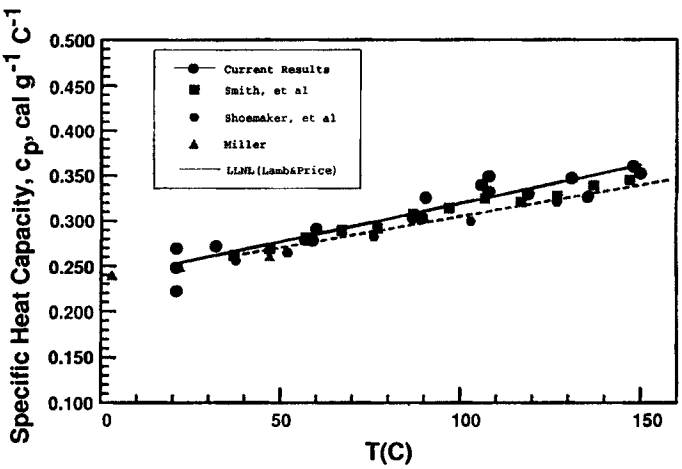

FIGURE 10.

Specific Heat Capacity of RDX.

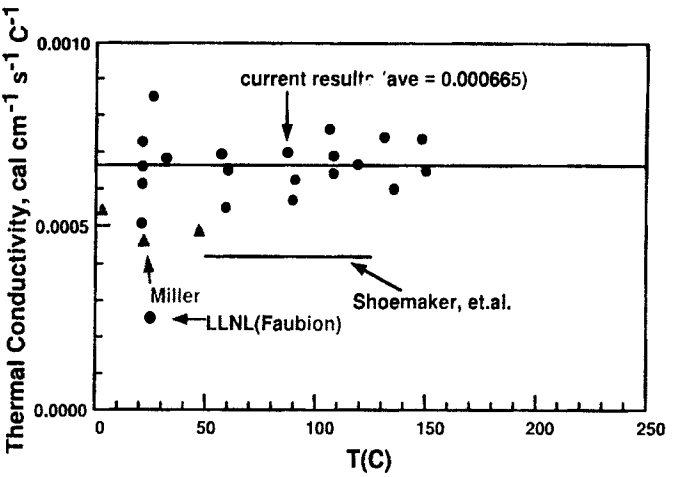

FIGURE 11.

Thermal Conductivity of RDX.

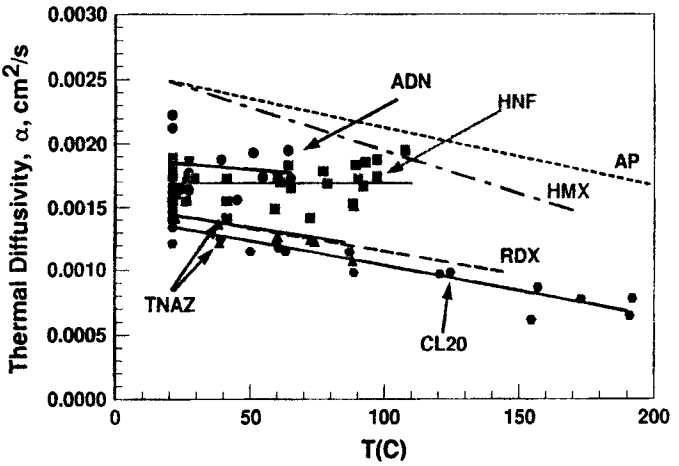

FIGURE 12.

Thermal diffusivity as a function of T(°C) for the oxidizers: AP, ADN, CL20, HMX, HNF, RDX, and TNAZ.

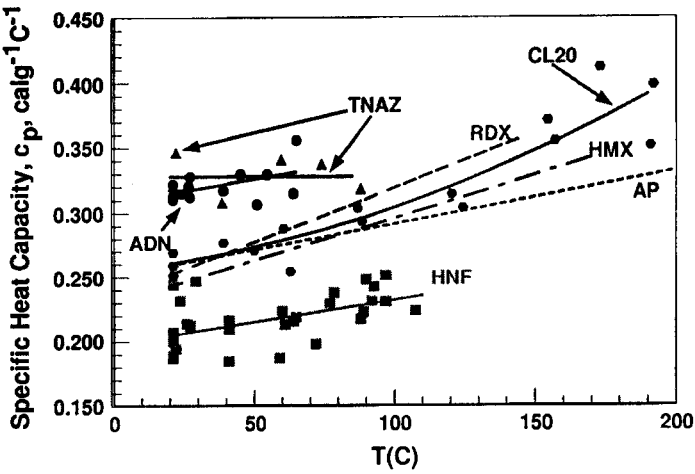

FIGURE 13.
Specific heat capacity as a function of T(°C) for the oxidizers: AP, ADN, CL20, HMX, HNF, RDX, and TNAZ.

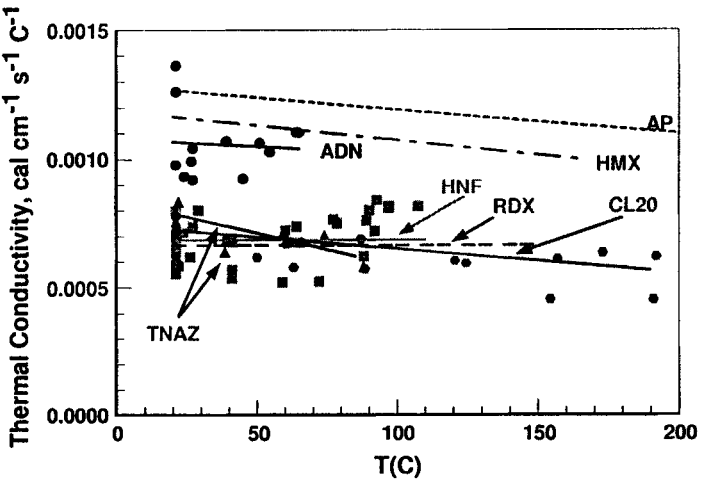

FIGURE 14.
Thermal conductivity as a function of T(°C) for the oxidizers: AP, ADN, CL20, HMX, HNF, RDX, and TNAZ.

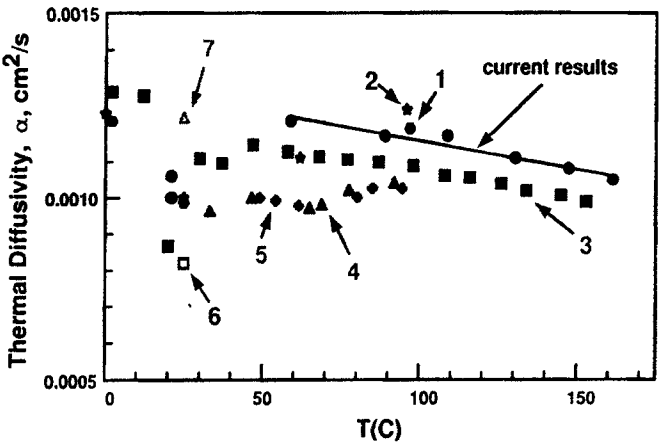

FIGURE 15.
Thermal diffusivity of Teflon™. The numbers on the curve refer to the numbered curves in ref. 6.

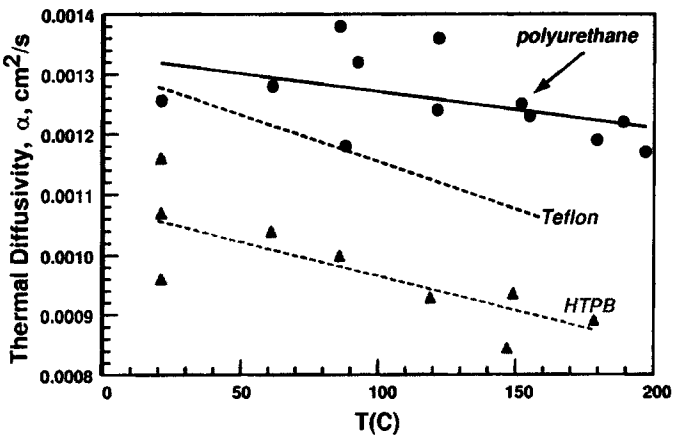

FIGURE 16.
Thermal diffusivities of the polymers Teflon™, HTPB, and polyurethane (isocyanate).

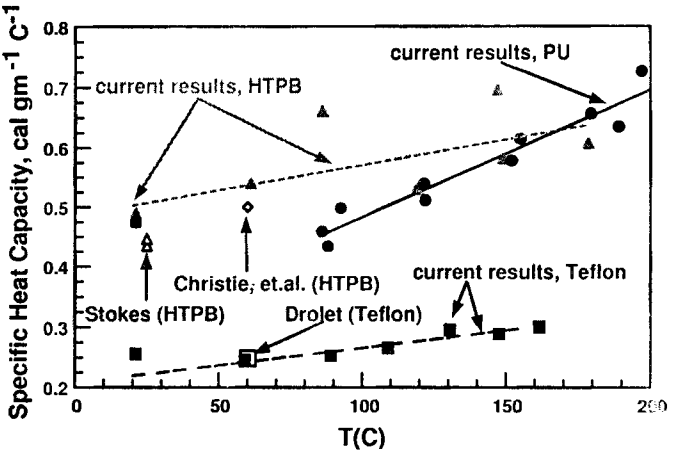

FIGURE 17.

Specific heat capacity of the polymers Teflon™, HTPB, and polyurethane (isocyanate).

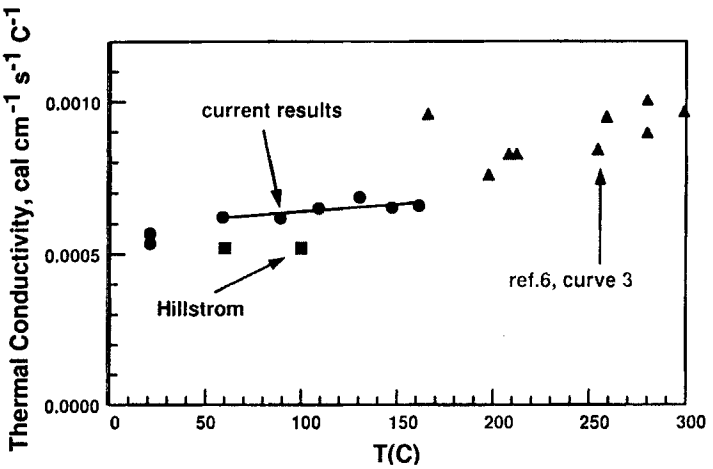

FIGURE 18.

Thermal conductivity of Teflon™.

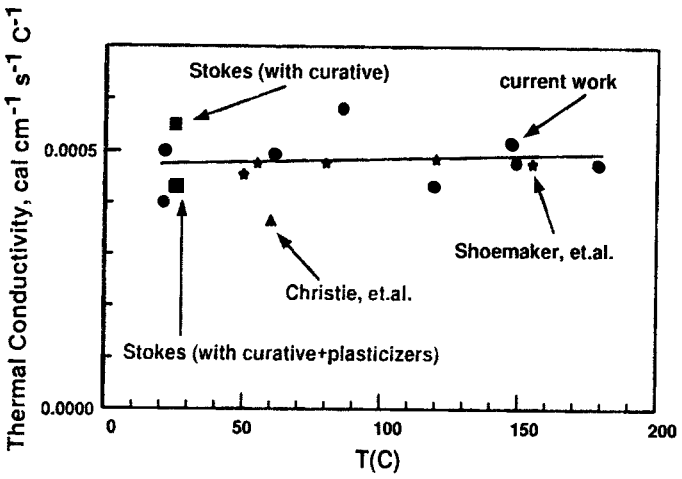

FIGURE 19.

Thermal conductivity of HTPB.

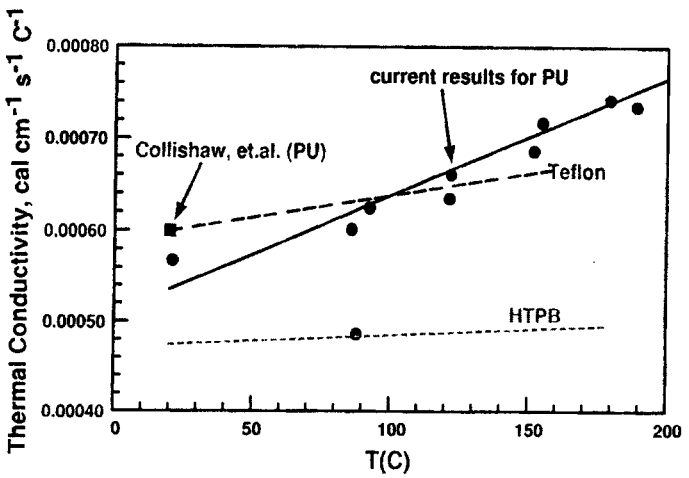

FIGURE 20.

Thermal conductivity of the polymers Teflon™, HTPB, and polyurethane (isocyanate).

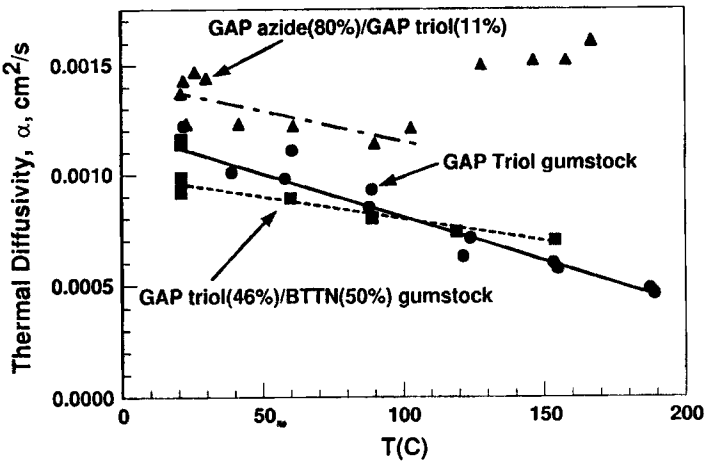

FIGURE 21.
Thermal diffusivity of GAP-based gumstocks.

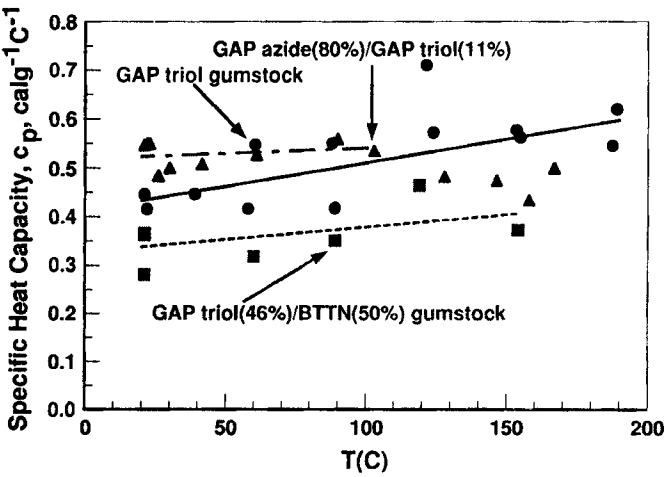

FIGURE 22.
Specific heat capacity of GAP-based gumstocks.

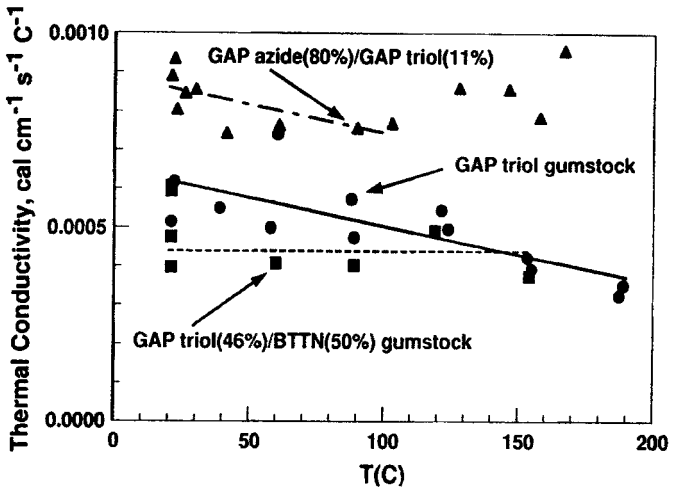

FIGURE 23.
Thermal conductivity of GAP-based gumstocks.

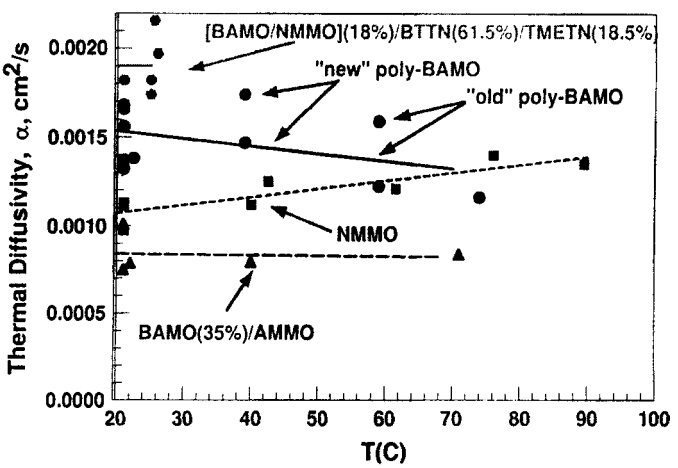

FIGURE 24.
Thermal diffusivities of BAMO- and/or NMMO-based polymers.

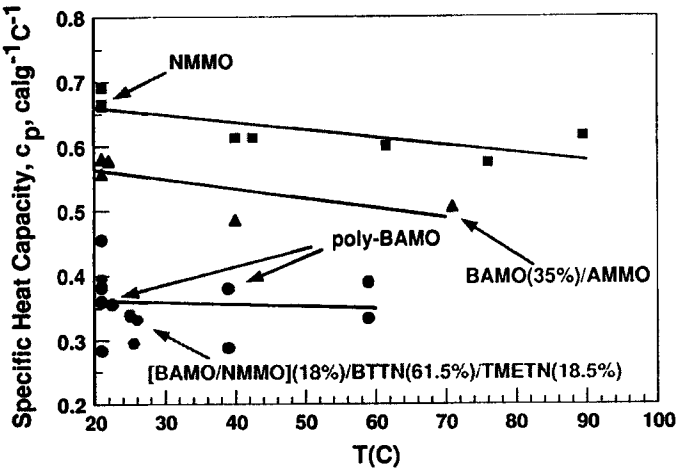

FIGURE 25.
Specific heat capacities of BAMO- and/or NMMO-based polymers.

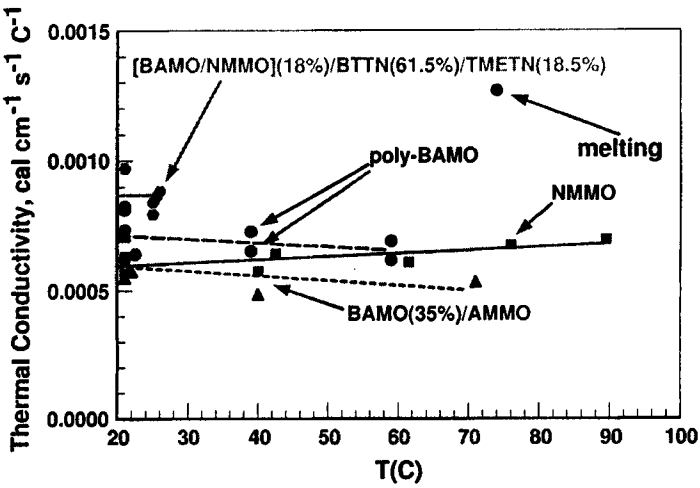

FIGURE 26.
Thermal conductivities of BAMO- and/or NMMO-based polymers.

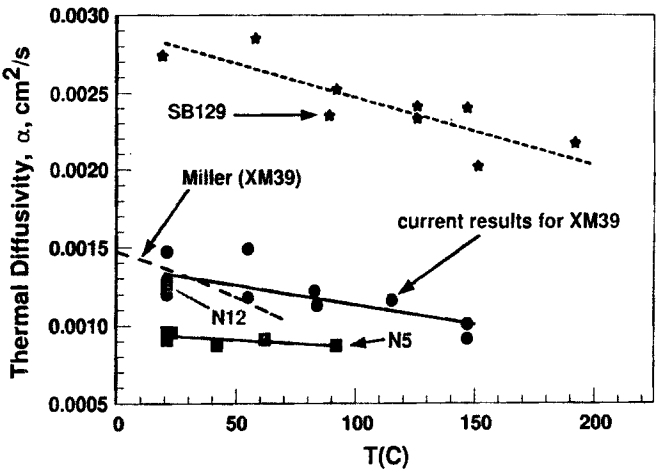

FIGURE 27.
Thermal diffusivity measurements for propellants.

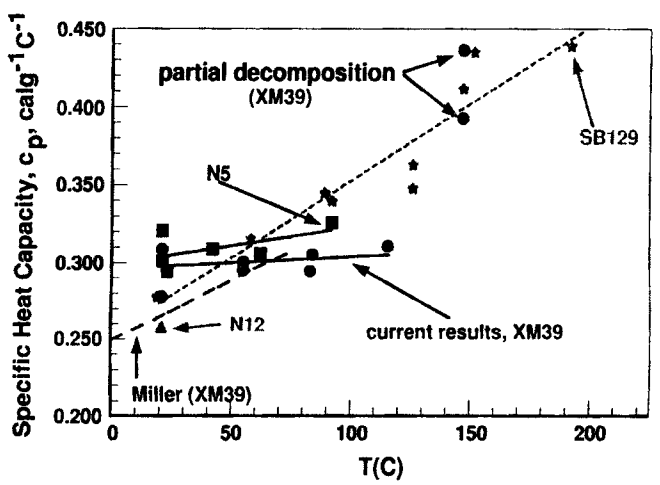

FIGURE 28.
Specific heat capacity measurements for propellants.

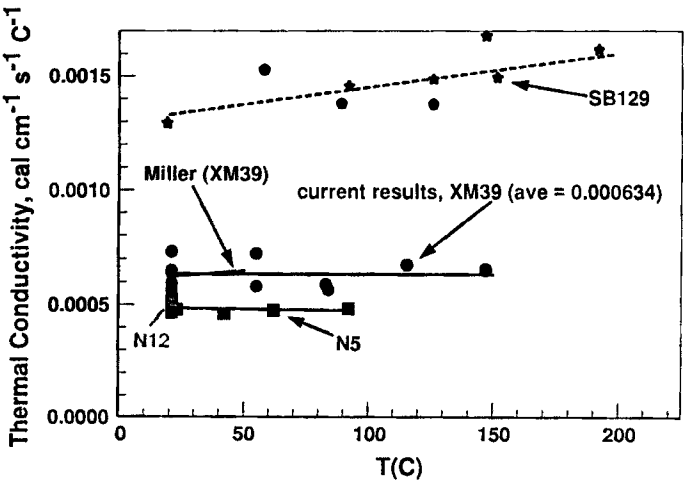

FIGURE 29.
Thermal conductivity measurements for propellants.